Imaging of Vascular Anomalies

Delma Y. Jarrett, MD*, Muhammad Ali, MD,
Gulraiz Chaudry, MB, ChB

KEYWORDS

• Vascular anomalies • Vascular malformation • Hemangioma • Imaging

KEY POINTS

- Vascular anomalies can be divided into two groups, tumors and malformations, on the basis of biologic behavior.
- Types of vascular tumors include infantile hemangioma and kaposiform hemangioendothelioma. Infantile hemangioma is seen as a well-defined mass with fast flow, whereas kaposiform hemangioendothelioma has poorly defined, infiltrative margins and is strongly associated with Kasabach-Merritt phenomenon.
- Low-flow malformations include venous and lymphatic malformations. LM can be subdivided into macrocystic, which demonstrate peripheral and septal enhancement, and microcystic, which appear more solid.
- Fast-flow vascular malformations include arteriovenous fistula and arteriovenous malformation. In arteriovenous fistula, there is a direct connection between the artery and vein, whereas in arteriovenous malformation, an intervening nidus is seen. Neither has an associated mass.

INTRODUCTION

Vascular anomalies comprise a diverse group of conditions in the pediatric and adult age group. The subject is often complicated by the use of improper descriptive terminology. Although the biologic classification proposed by Mulliken and Glowacki in 1982[1] and later adopted by the International Society for the Study of Vascular Anomalies[2] substantially helped to resolve this dilemma, vague terminology continues to be used in the clinical setting and medical literature. Accurate characterization of vascular anomalies is crucial in predicting the clinical course, prognosis, and need for intervention. It is therefore important to adhere to a standard classification system in clinical assessment and radiologic characterization.

Mulliken and Glowacki divided vascular anomalies into two groups: hemangiomas and malformations, with the first category later expanded to include multiple vascular tumors in addition to hemangiomas. This distinction is based on endothelial cell characteristics. Vascular tumors consist of proliferating cells with increased mitotic activity. Malformations arise from abnormal vascular channels in the absence of abnormally proliferating endothelium.[1,3]

Infantile hemangiomas (IH) are the most common type of vascular tumor; however, they must be distinguished from other vascular tumors including rapidly involuting congenital hemangiomas (RICH), noninvoluting congenital hemangiomas (NICH), kaposiform hemangioendothelioma (KHE), and tufted angioma.

Vascular malformations can be further divided into slow-flow, fast-flow, and mixed lesions. Slow-flow lesions include capillary, venous, and lymphatic malformations (LM). Fast-flow lesions are arteriovenous malformations (AVM) and arteriovenous fistulas (AVF).

IMAGING

Although the diagnosis can sometimes be made clinically, radiologic assessment is often helpful

Harvard Medical School, Department of Radiology, Boston Children's Hospital, 300 Longwood Avenue, Boston, MA 02115, USA
* Corresponding author.
E-mail address: delma.jarrett@childrens.harvard.edu

Dermatol Clin 31 (2013) 251–266
http://dx.doi.org/10.1016/j.det.2012.12.004
0733-8635/13/$ – see front matter

in the management of vascular anomalies, particularly for atypical or deep lesions, and is important for treatment planning. Ultrasound (US) and magnetic resonance imaging (MRI) are the mainstay of imaging vascular anomalies, with limited roles for radiography and computed tomography (CT).

US is a relatively accessible, noninvasive modality that can be performed in the often young patient population without sedation or ionizing radiation. With gray-scale imaging, the vascular anomaly can be characterized as cystic, composed of channels, or as a solid mass with well or poorly defined margins. Calcifications can be identified as echogenic foci with posterior shadowing. With Doppler imaging, one can assess for the presence and distribution of blood flow to the lesion. Spectral waveforms can determine if the flow is arterial or venous, and assess for the presence of shunting. Skin lesions should be imaged with a high-frequency linear transducer, although deeper lesions necessitate lower-frequency transducers.

MRI is superior to US in evaluating the extent of the lesion, including the tissue planes and adjacent structures involved. Routine sequences include short time inversion recovery (STIR)/T2-weighted images with fat saturation (FS), which for most vascular anomalies provide sharp contrast between the lesion and normal tissue. Depending on the appearance of these fluid-sensitive sequences, T1-weighted FS postcontrast images may be useful to assess perfusion to the anomaly. MR angiography (MRA) is sometimes helpful in the assessment of fast-flow vascular anomalies. Techniques include noncontrast imaging angiography using two-dimensional time-of-flight or phase-contrast imaging, or dynamic imaging with gadolinium-enhanced time resolved MRA, which allows the arterial and venous phases to be imaged separately, demonstrating feeding arteries, draining veins, and location of shunts. Large vessels can be imaged using spin echo (SE) sequences, where they appear as signal voids, or gradient recall echo (GRE) sequences, where vessels are bright. GRE images also demonstrate calcification and blood products, either from bleeding of the anomaly or from thrombus.

Radiographs may be used to assess the bony changes associated with vascular anomalies. These are almost always related to malformations rather than hemangiomas and include periosteal reaction, well-defined lucent lesions in the bone, leg length discrepancy, and overgrowth of the affected side.[4] CT is largely reserved for accurate evaluation of bone destruction.

VASCULAR TUMORS

Infantile Hemangiomas

Background and clinical presentation

IH are the most common tumors of infancy, with risk factors including fair skin, prematurity, and female gender.[5] They are most commonly found in the head and neck region, followed by the trunk, then the extremities. Subtle skin findings are sometimes present at birth, although in most cases the diagnosis is made at 2 to 4 weeks of age. IH then typically undergo a 6- to 8-month period of rapid growth in neonatal life, plateauing at 10 to 12 months, followed by a period of involution lasting 1 to 7 years.[3]

The cutaneous manifestation depends on the depth of the tumor, with superficial lesions appearing raised and red (“strawberry appearance”), whereas the overlying skin can be normal with deeper lesions.[6]

Radiologic imaging

Ultrasound The US appearance of IH depends on whether it is in the proliferating to plateau phase or the involuting phase. In the earlier phases, it appears as an echogenic, well-circumscribed soft tissue mass. Gray-scale imaging can occasionally demonstrate anechoic channels, corresponding to the high-flow vessels. Color Doppler imaging is better at demonstrating the vascularity, with high vessel density seen (five or more vessels in a square centimeter), and arterial and venous waveforms obtained (**Fig. 1**A, B).[6,7] Involuting IH are rarely imaged because they are unlikely to present a diagnostic dilemma at that stage, but have been described as isoechoic, difficult to differentiate from adjacent soft tissues, and with no demonstrable blood flow.[7]

Magnetic resonance imaging The MRI appearance of IH also depends on its stage of growth. During the proliferative and plateau phase, they are seen as focal, lobulated soft tissue masses that are isointense to muscle on T1-weighted images, hyperintense on T2-weighted images, and demonstrate homogeneous enhancement (see **Fig. 1**C–F).[8,9] SE and GRE sequences demonstrate enlarged high-flow vessels within the mass, although intralesional flow voids may be difficult to discern in early infancy. These features can help to distinguish IH from other tumors, such as sarcomas, which tend to enhance heterogeneously, and have a more random distribution of vessels.[8]

Histologically, involuting IH are replaced by fibrofatty tissue. This is reflected in their MRI appearance, where they follow the signal intensity of the surrounding fat. There is also a decrease in enhancement and visualized vessels.[8]

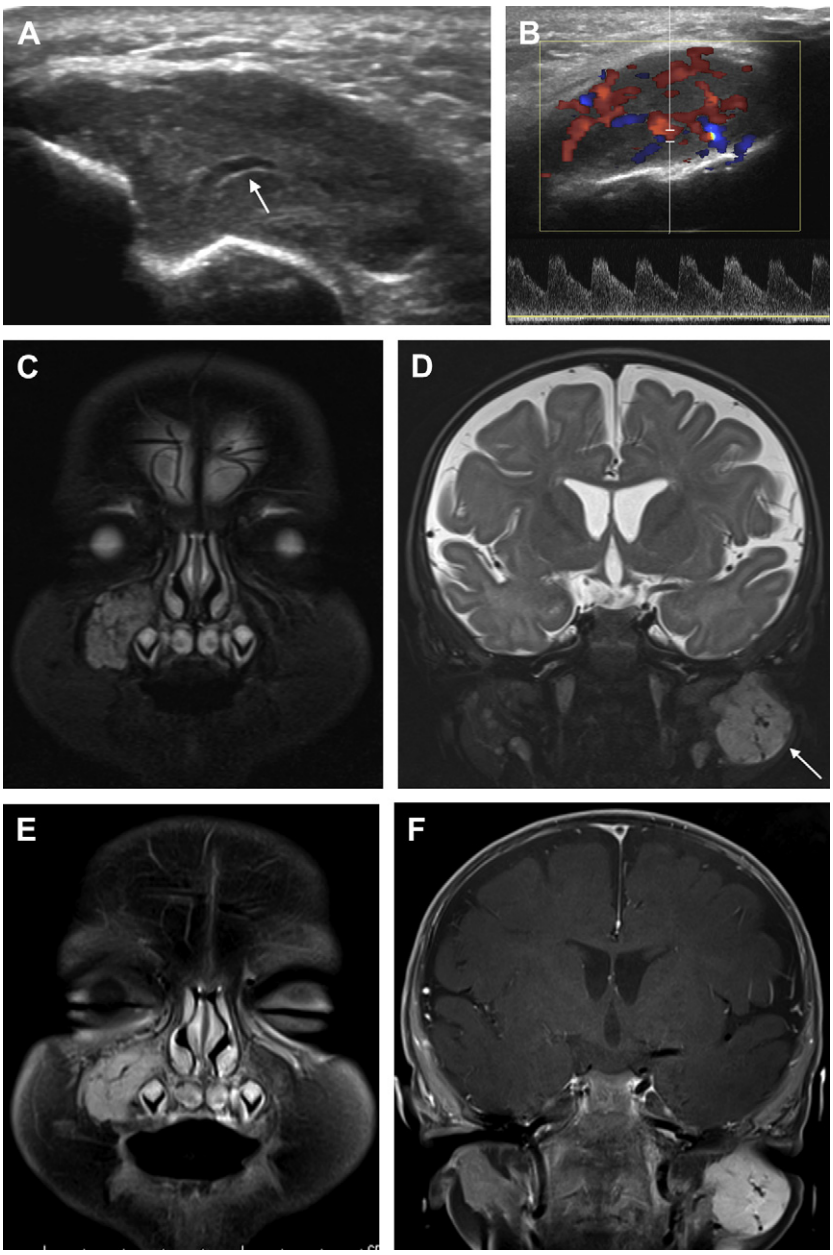

Fig. 1. Infantile hemangiomas in a 3-month-old girl who presented with mass under her right eye. (*A*) Ultrasound image of the right face lesion demonstrates a well-defined mass in the subcutaneous tissues, abutting the underlying bone, with hypoechoic channels corresponding to vessels (*arrow*). (*B*) Color Doppler image confirms that the mass is hypervascular, with low-resistance arterial waveforms. MRI was performed at 4 months of age. Coronal STIR images again show the mass below the right eye (*C*) and a second IH involving the left parotid gland (*D, arrow*). Both are hyperintense on fluid-weighted sequence with dark flow voids corresponding to vessels. After intravenous contrast administration the IH of the right face (*E*) and left parotid (*F*) demonstrate homogenous enhancement.

Angiography Angiographically, IH appear as well-circumscribed masses, with a lobular pattern of intense tissue staining. They are supplied by slightly enlarged but otherwise normal branches of systemic arteries, demonstrate a distinct tumor blush, and are drained by small veins that communicate with dilated but otherwise normal local veins. Typically, no direct AV shunting is seen within the mass.[10]

Imaging associations In certain cases, additional imaging is required to screen for other potential anomalies. The presence of five or more

cutaneous hemangiomas raises suspicion for the presence of visceral, particularly liver, hemangiomas. These infants should be screened by US or MRI.[3] Large cervicofacial hemangiomas in a "beard" distribution are associated with subglottic airway hemangiomas, which in addition to direct imaging by endoscopy can be imaged MRI, CT, and high-resolution US.[11–13] Large facial hemangiomas are associated with PHACE syndrome.[13,14] Those in the lumbosacral region are associated with spinal anomalies including tethered cord, spinal lipoma, and intraspinal hemangioma, and with SACRAL and LUMBAR syndromes (**Table 1**).[15–17]

Treatment and complications

Because IH spontaneously involute, most do not require treatment. However, medical therapy may be indicated if the location of the hemangioma compromises vision or the airway. Currently, the first line of treatment is oral administration of propranolol or steroids. In addition, if multifocal hepatic hemangiomas are identified, thyroid-function testing should be performed as soon as possible. The triiodothyronine deiodinase produced by these tumors peripherally deactivates T3 and these infants often require large doses of thyroid hormone replacement for correction.[18] Intralesional injections, embolization, and resection are generally reserved for a small minority of hemangiomas causing significant cosmetic deformity or cardiac failure.

Congenital Hemangiomas

Clinical presentation

In contrast to IH, CH reach their maximum size at the time of birth and can sometimes be diagnosed prenatally. Unlike IH, there is no gender predilection and the tumors do not test positive for glucose transported protein 1.[19] CH demonstrate two patterns of clinical progression. Most undergo rapid postnatal involution, resolving by 14 months of age, as a RICH. Alternatively, the CH never regresses and continues to grow proportionately with the child, and is called NICH.[20] Some of the lesions demonstrate initial rapid decrease in size and then plateau and remain unchanged. Therefore, it is possible that NICH represents a later stage of RICH in some patients.[19]

CH are usually solitary and often involve the head or the limbs near a joint.[20,21] The involved skin is usually blue or violaceous, with telengiectasias; a pale peripheral halo is more characteristic of NICH than RICH.[22]

Radiologic imaging

Ultrasound The sonographic findings in CH are often similar to IH, with a fast-flow soft tissue mass seen in both cases (**Fig. 2**). Features more suggestive of CH are heterogeneity, calcifications, and increased conspicuity of intralesional vessels.[21]

RICH and NICH cannot initially be easily distinguished from each other by US. However, as they involute, RICH are characterized by tortuous compressible channels demonstrating venous flow. These correspond to the histologic finding of thin-walled drainage channels separated by fibrous tissue.[23] NICH are more likely to demonstrate microshunting,[21] manifested as increased turbulence or pulsatility in the venous waveforms.

Magnetic resonance imaging CH are isointense on T1- and hyperintense on T2-weighted images,

Table 1
Syndromes associated with infantile hemangiomas

Syndrome		IH Distribution
PHACE	Posterior fossa brain malformation Hemangiomas Arterial anomalies Coarctation of the aorta and cardiac defects Eye abnormalities	Large, facial
LUMBAR	Lower body IH and other skin defects Urogenital anomalies and ulceration Myelopathy Bony deformities Anoretal malformations, Arterial anomalies Renal anomalies	Extensive of lower half of body, often involving entire limb
SACRAL	Spinal dysraphism Anogenital Cutaneous Renal and urologic anomalies, associated with an angioma of lumbosacral localization	Perineal

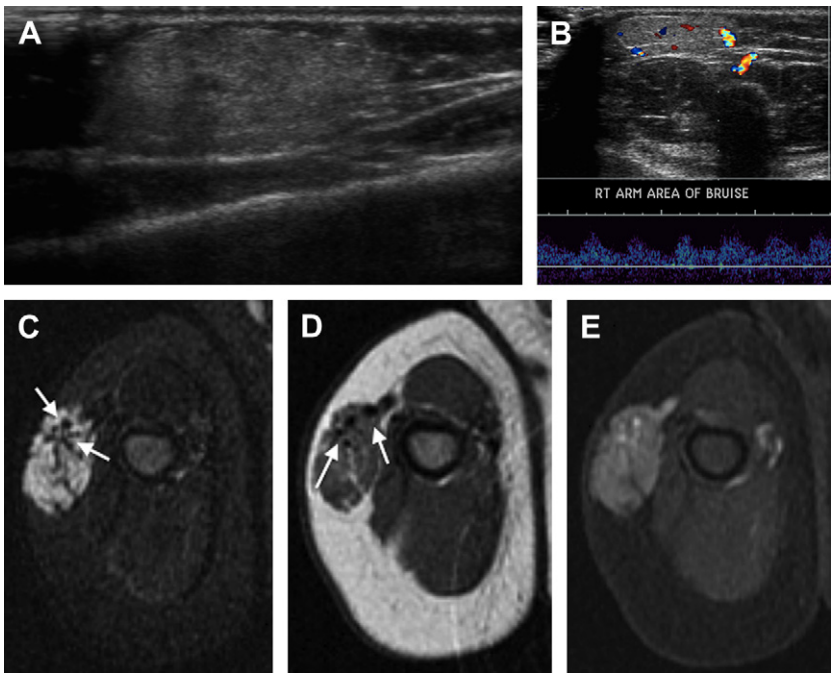

Fig. 2. RICH in 6-month-old boy with multiple vascular birthmarks, which rapidly regressed in the first yew years of life. (*A*) Sagittal ultrasound image of a right arm lesion shows a hyperechoic mass in the subcutaneous tissues. (*B*) Transversely oriented ultrasound image of the mass with color Doppler shows internal vascularity, with low-resistance arterial waveforms. MRI was performed at 8 months of age. Axial STIR (*C*) and axial T1 images (*D*) through the right arm lesion show a lesion that is hyperintense on the fluid-weighted sequence with prominent flow voids related to intralesional vessels (*arrows*). (*E*) On T1 FS image, after administration of intravenous gadolinium, there is homogeneous enhancement.

with intense enhancement after contrast administration. They are more likely to have heterogeneous enhancement and poorly defined borders than IH, although they still lack surrounding edema, which can be seen in more aggressive lesions (**Fig. 3**).[21] On SE and GRE sequences, feeding and draining vessels can be seen.

Angiography NICH demonstrate arterial feeding vessels, with tumor-like capillary blush. They have dilated draining veins as can be seen with AVF or AVM (**Fig. 3**). However, unlike these entities, NICH do not demonstrate early venous drainage.[20]

Because of their natural history, RICH are less likely to be assessed angiographically, but do demonstrate inhomogenous parenchymal staining; large, irregular, and disorganized feeding arteries; direct AV shunts; and intravascular thrombi.[24]

Complications and treatment

Because of the rapid involution in most RICH cases, no treatment is required. In a few cases, there is redundant skin after involution with central fissuring and ulceration, which necessitates surgical resection.[22] NICH are surgically resected.

Kaposiform Hemangioendothelioma

Background and clinical presentation

KHE is a rare vascular lesion that can be congenital, with 50% presenting at birth in one series,[25] but can also present later in childhood.[26] They grow rapidly, and are locally aggressive, but have been seen to spontaneously regress.[25,27,28] There is no gender preference. They often involve the trunk, extremities, retroperitoneum, and rarely the cervical/facial region. The overlying skin is red to purple in color with a rim of ecchymosis, and is warm and edematous to palpation.[25] Importantly, there is a frequent association with Kasabach Merritt phenomenon (KMP), a consumptive coagulopathy,[25] with 90% of cases of KMP occurring secondary to KHE.[26]

Ultrasound

On US, KHE has variable echogenicity. The margins are ill defined, a major distinguishing characteristic from IH (**Fig. 4**A, B). They may also contain foci of calcification, a feature not seen in IH. Although there have been reports of decreased vessel density compared with IH, color Doppler imaging characteristics cannot reliably differentiate the two lesions.[28]

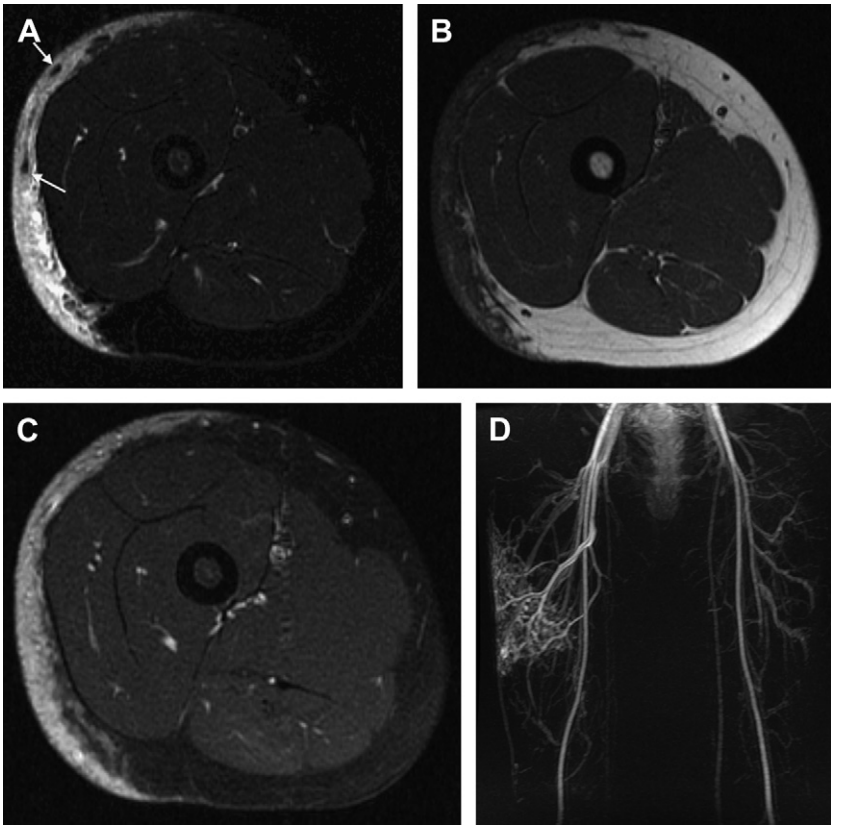

Fig. 3. NICH in 8-year-old girl born with purple birthmark on her right thigh, which grew proportionately with her. (*A*) Axial T2 FS image through the right thigh shows mass in the anterior subcutaneous tissues with poorly defined margins. It contains flow voids from prominent intralesional vessels (*arrows*). The mass is hypointense on T1 image (*B*) and demonstrates diffuse enhancement on T1 FS postcontrast image (*C*). (*D*) MR angiogram shows numerous prominent feeding arteries, draining veins, and tumor-like blush of the mass.

On MRI, KHE are seen as soft tissue masses that are hypointense to isointense to muscle on T1-weighted images, and heterogeneously hyperintense on T2-weighted images. They are infiltrative, extending to involve multiple tissue planes, with ill-defined borders, stranding in the subcutaneous tissues, and overlying skin thickening. On postgadolinium T1-weighted images, the tumor demonstrates a strong reticular enhancement pattern, corresponding to the same pattern seen on T2-weighted images (**Fig. 4**C–E). Associated prominent vascular channels are seen either on postcontrast images or as flow voids on SE sequences.[25,29] Compared with IH where the size of the feeding and draining vessels is proportional to the size of the tumor, the vessels of KHE are small relative to tumor size. KHE may contain hemosiderin, blood products, or fibrosis,[25] which are best demonstrated on GRE images.

Complications and treatment

There is significant mortality associated with KHE, ranging from 10% to 30%, with the rate higher for retroperitoneal tumors.[25–27] This is caused by the sequela of local invasion and the high association with KMP. The mainstay of treatment is medical therapy with agents including vincristine, corticosteroids, ticlopindine, interferon-α,[30] and propranolol.[27] Surgical resection may be possible in localized cases.

SLOW-FLOW VASCULAR MALFORMATIONS

Venous Malformation

Background and clinical presentation

VM are congenital malformations characterized by dilated venous channels deficient in smooth muscle. These channels also lack normal valves and have stagnant flow.[31] VM may take many different forms, ranging from varicosities and ectasias to complex channels and localized spongiform masses.[3]

Like all vascular malformations, they are present at birth. VM do not regress and grow proportionately with the patient, with periods of enlargement during puberty and pregnancy because of hormonal influence. On physical examination, VM

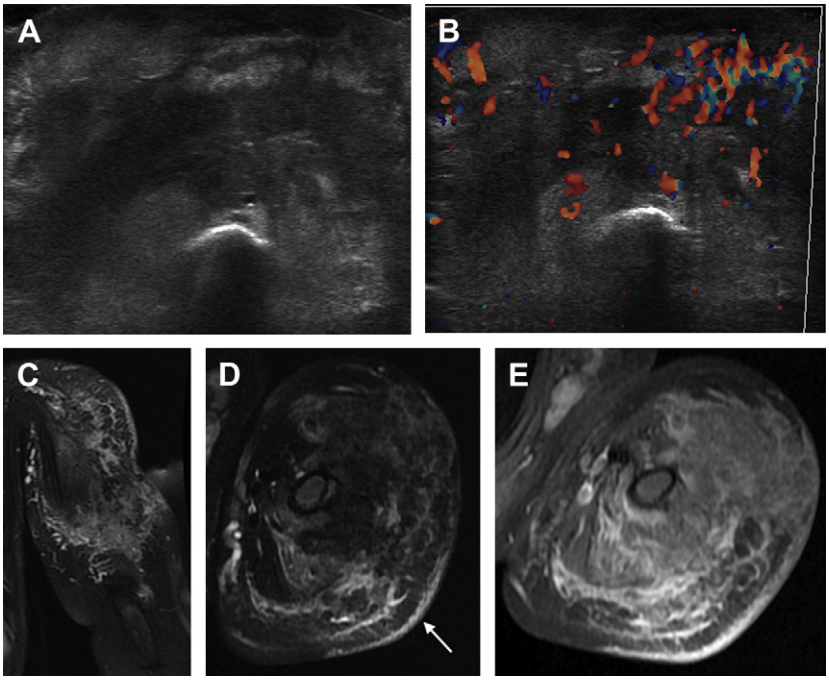

Fig. 4. KHE in the upper left arm of an 11-month-old boy. (*A*) Transverse US mage shows poorly defined heterogeneous soft tissue mass of the arm. (*B*) Color Doppler demonstrates hypervascularity. Coronal (*C*) and axial (*D*) T2 FS images demonstrate an infiltrative hyperintense lesion involving multiple tissue planes, with areas of skin thickening (*arrow*). (*E*) Axial T1 FS postcontrast images show heterogeneous enhancement.

are soft, compressible, and nonpulsatile. The overlying skin may be normal or have a bluish tinge. Maneuvers that increase venous pressure (dependant position, crying, Valsalva) cause them to increase in size.[32,33] VM most commonly involve the head and neck, followed by the extremities, with truncal involvement less frequently seen. Although skin involvement is common, VM can extend to or have isolated involvement of muscle, bone, and abdominal organs.[34]

Radiographic imaging

Ultrasound There is a varied US appearance of VM that reflects the different morphologies of this entity, ranging from the hypoechoic or heterogeneous spongiform appearance of localized cavernous spaces, to anechoic vascular channels of dysplastic veins (**Fig. 5**).[7,33,35] When Doppler flow is present, it is monophasic, low-velocity flow.[33] Twenty percent of VM show no flow on Doppler imaging because of either undetectably slow flow or true lack of flow secondary to thrombosis.[34] In this case, the lack of cystic cavities can help distinguish them from LM.[33] Phleboliths can be seen as hyperechoic, shadowing foci.

Magnetic resonance imaging STIR or T2 FS sequences are the most useful to assess the extent of the lesion, which can often be underestimated on clinical examination. VM appear as hyperintense on T2-weighted images and hypointense on T1-weighted images (**Fig. 5**). With hemorrhage or thrombosis, the VM may demonstrate increased heterogeneous signal on T1-weighted images.[34,36] Fluid-fluid levels can be seen in regions of low or no flow. These malformations commonly extend from the subcutaneous fat to involve muscle and fascia, sometimes involving the bone, tendons, and joints. In the extremities, they tend to be oriented along the long axis, parallel to fascial planes.[31] The characteristic phleboliths of VM and potential blood products/hemosiderin are best seen on GRE sequences.

Postcontrast, there is often marked but heterogeneous enhancement.[34,36] On SE sequences, there are no flow voids, as can be seen with high-flow vascular anomalies.[36] No prominent feeding artery or draining vein is seen.[31] Although two-dimensional time-of-flight venography may demonstrate dysplastic veins, it is rarely required to either establish a diagnosis or guide further management.

Initial assessment of VM should include a wide field of view, to assess the full extent of the lesion. This is important because incomplete resection of a VM can cause flare in size and symptoms of the residual malformation.[31]

MRI may also demonstrate soft tissue changes related to the VM, such as fatty replacement,

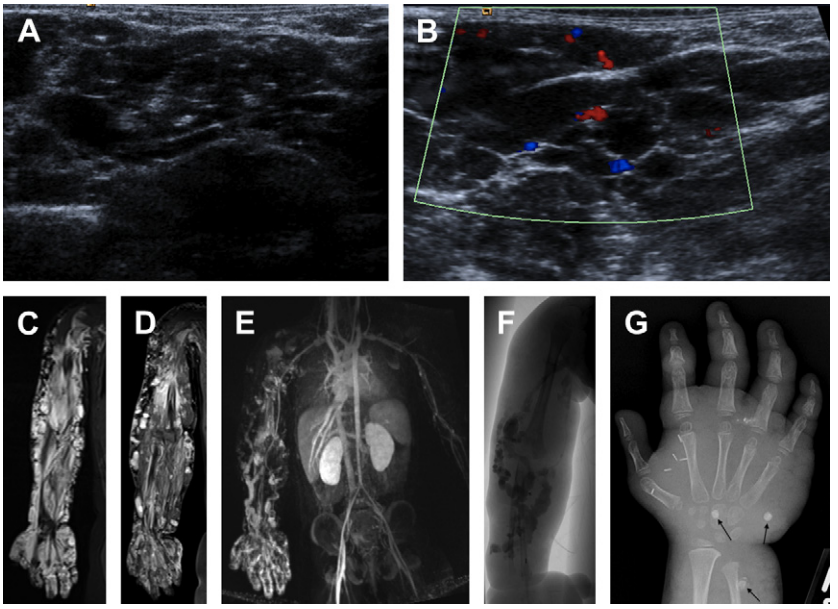

Fig. 5. Young girl with extensive venous malformation of the right arm. US images obtained at 3 years of age demonstrate a hypoechoic, spongiform malformation (*A*) with little flow seen on color Doppler (*B*). MRI also obtained at 3 years of age. Fluid-weighted (*C*) and postcontrast (*D*) sequences demonstrate hyperintense tubular and lobulated structures involving all the soft tissue layers with heterogeneous enhancement after contrast. Post-contrast MRI (*E*) and conventional venography (*F*) clearly demonstrate the associated abnormal ectatic veins. (*G*) Radiograph of the right hand shows multiple phleboliths (*arrows*).

atrophy of the adjacent musculature, or hypertrophy of the subcutaneous fat compared with the contralateral side.[31]

Angiography Angiographic evaluation of VM is best performed with direct intralesional injection of contrast. With arterial injection, normal arteries are seen with no evidence of AV shunting. There is also limited assessment of the VM, because of poor opacification of proximal veins caused by slow flow.[35,36] Therefore, there is no role for arteriography in the diagnosis or management of VM.

Direct venography and intralesional injection are sometimes better in characterizing the VM, but visualization is limited to the cannulated vessels and associated draining vein (**Fig. 5**F).[36] Using US guidance, a needle is advanced into the VM and a small volume of low osmolarity iodinated contrast is injected. Based on the venographic findings, some have characterized the VM as one of four types: (1) isolated VM with no visible draining veins, (2) drainage into normal veins, (3) dysplastic draining veins, and (4) venous ectasia. Type 3 or 4 lesions are higher risk for sclerotherapy because of the potential for distal embolization.[32,37]

Radiographs and CT Radiographs may reveal the presence of a soft tissue mass or phleboliths, which are highly suggestive of VM (**Fig. 5**G). However, the main use of radiographs and CT is in assessing skeletal manifestation of VM, such as direct osseous involvement or associated bony overgrowth. The malformations appear as hypodense or heterogeneous in density, with slow, peripheral enhancement. CT is not as helpful as MRI in characterizing the type or extent of the lesion.[34] Extension of the malformation into the deep musculature and bone is best appreciated on MRI. Therefore, there is no role for routine use of CT in the assessment of VM.

Treatment and complications

VM are referred for treatment because of pain, cosmetic issues, or loss of function caused by location. They can cause localized intravascular coagulopathy, which is a separate entity from KMP.[3] Sclerotherapy is the primary treatment in most cases, with agents including Ethibloc (Ethnor Laboratories/Ethicon, Norderstedt, Germany), sodium tetradecyl sulfate, and absolute alcohol.[37] Direct injection and venography are performed before sclerotherapy to assess the VM and the deep venous anatomy. Local complications of sclerotherapy include skin necrosis, ulceration, and peripheral nerve damage. Rare systemic complications can occur if ethanol passes into the systemic circulation, causing hemolysis, renal toxicity, and cardiac arrest.[34]

Multiple treatments are often necessary. Interim MRI can be performed to assess response to treatment but there should be a delay between sclerotherapy and repeat imaging of several months to allow posttreatment inflammation to resolve. After treatment, the VM usually demonstrates increased heterogeneity on T1- and T2-weighted images and decrease in size. Postcontrast imaging can show potential areas of residual perfusion.[34] However, because the diagnosis is already established, the use of contrast is rarely necessary. Surgical resection may be performed if sclerotherapy does not provide adequate results.

Lymphatic Malformation

Background and clinical presentation

LM result from disordered development of the lymphatic system. Dilated lymphatic channels lack normal communication to the lymphatic system.[38] Depending on the size of these spaces, they can be characterized as microcystic, macrocystic, or mixed. There is considerable variability in the criteria used to designate a malformation as microcystic or macrocystic. At our institution, only lesions or parts of lesions containing cysts that are too small to be accessed and aspirated with a hypodermic needle are designated as microcystic.

Although congenital, only 50% of LM are seen at birth, with 90% diagnosed by the age of 2.[39] A total of 70% to 80% involve the head-neck region.[40] They usually present as asymptomatic masses, which enlarge because of hemorrhage or infection. The overlying skin usually appears normal, but may have capillary staining or cutaneous blebs or vesicles, which are pathognomonic for LM.[3] A small minority have been reported to spontaneously regress.[41]

Radiologic imaging

Ultrasound Macrocystic LM appear as cysts, sometimes containing echogenic debris. No blood flow is identified within the cavities themselves, although small arteries and veins may be seen within the cyst walls or intervening stroma (**Fig. 6**A).[7] In microcystic LM, the individual cysts are too small to discern. They appear as echogenic regions with soft tissue thickening (**Fig. 7**A).

Magnetic resonance imaging Macrocystic LM are isointense to hypointense on T1-weighted and hyperintense on fluid sensitive/T2-weighted images (see **Fig. 6**). Fluid-fluid levels are common, especially when there is associated hemorrhage. They demonstrate no or minimal peripheral enhancement involving the cyst walls. The venous channels are usually normal, although occasionally large or anomalous veins can be seen.[8,42]

As on US, the individual cysts of microcystic LM cannot be discerned. They appear as a region of diffuse hypointense signal on T1-weighted images and hyperintense on T2-weighted images. Microcystic LM can on occasion show mild diffuse enhancement, which can lead to confusion with a solid mass (see **Fig. 7**).[8]

Complications and treatment

In the extremity, LM can cause local gigantisim, with bony and soft tissue overgrowth. Diffuse LM of the chest can cause chronic chylous effusion, and in the gastrointestinal tract a protein-losing enteropathy. In Gorham-Stout disease, LM of the bone and surrounding soft tissue causes osteolysis.[3]

The two most common complications are bleeding and hemorrhage.[3] LM can cause significant morbidity depending on the area of involvement (eg, causing mass effect on the trachea in neck and mediastinal involvement, or speech difficulties if the tongue is involved). Treatment options include sclerotherapy and surgical resection. Sclerotherapy is primarily effective for macrocystic LM, or the macrocystic component of a mixed lesion, with agents including bleomycin, Ethibloc, ethanol, OK-432 (Chugai Pharmaceutical Co, Ltd, Tokyo, Japan), doxycycline, and sodium tetradecyl sulfate.[39,41,43] Microcystic LM has a much less favorable response to sclerotherapy, although there have been encouraging reports with the use of intralesional bleomycin.[44,45] Complete resection is more easily accomplished with macrocystic LM than the more infiltrative and diffuse microcystic LM.[39] When possible, microcystic LM are managed conservatively.

FAST-FLOW LESIONS: AVM AND AVF

Background and Clinical Presentation

AVM are rare, resulting from an error in vascular development. They are composed of a nidus of anomalous connections between arteries and veins without intervening capillary bed. Like all vascular malformations, they are present at birth, although they may not be clinically apparent until later. On examination, AVM may present as a pulsatile mass with thrill, warmth, and redness.[8] Clinically, they can be categorized according to the Schobinger classification: stage 1, quiescence; stage 2, expansion (with enlargement of the AVM); stage 3, destruction (skin ulceration and bleeding); and stage 4, decompensation (cardiac failure).[46,47]

AVM expand over time, not because of cellular proliferation, but related to increased blood flow and the recruitment of adjacent normal vessels by shunts across the low-resistance arteriovenous

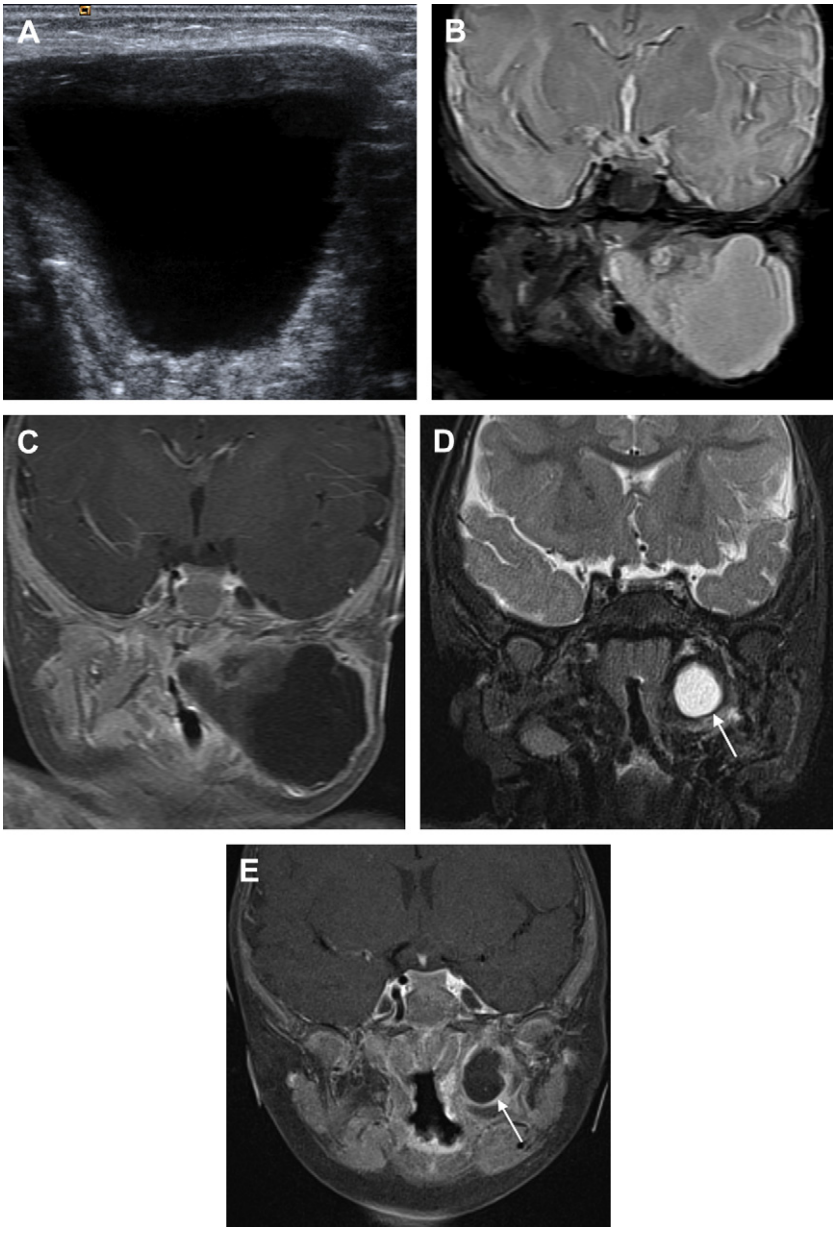

Fig. 6. Macrocystic LM in a 2-month-old girl who presented with upper airway obstruction. (*A*) US shows large anechoic cyst. (*B*) Coronal fluid-sensitive sequence demonstrates a hyperintense macrocystic lesion, with more complex lower-intensity component medially, reflecting hemorrhage. (*C*) Postcontrast coronal T1 FS image shows only peripheral enhancement. Patient underwent three sclerotherapy treatments with doxycycline, with significant decrease in size of the LM as seen on coronal FSEIR (*D*) and T1 FS postcontrast (*E*) images (*arrow*).

connections. Like VM, puberty and pregnancy can cause progression of the lesion.[47] AVM can also enlarge because of trauma, including the iatrogenic trauma of biopsy, ligation, or partial excision.[8,47]

AVF may be congenital or posttraumatic. Unlike AVM, there is usually a single arteriovenous communication present. However, if long-standing, AVF can also recruit additional vessels, simulating AVM.[48]

Radiologic Imaging

US imaging shows no soft tissue mass. Multiple, enlarged subcutaneous arteries and veins are present, with high-flow, low-resistance wave forms in the arteries and arterialized wave forms in the draining veins.[7,8]

Similarly on MRI, the dominant feature of AVM and AVF are the dilated, often tortuous feeding

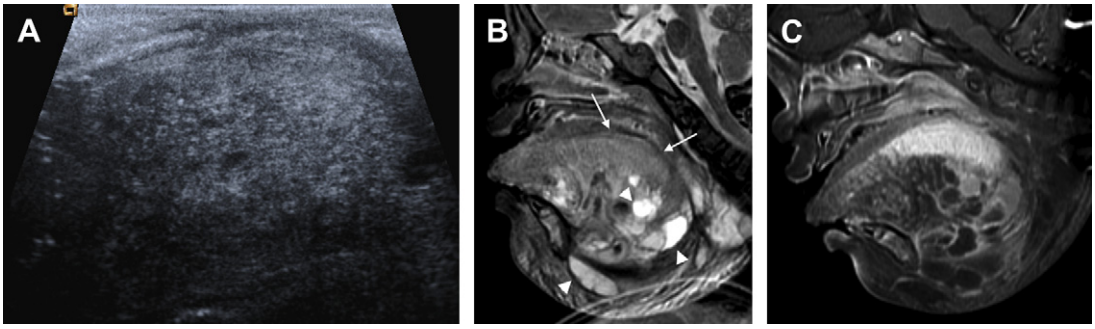

Fig. 7. A 2-year-old girl with microcystic LM of the tongue. (*A*) Ultrasound of the tongue shows heterogenous echotexture with innumberable hyperehcoic foci corresponding to the walls of the microcysts. Sagittal T2 FS image (*B*) shows soft tissue thickening and increased T2 signal within the tongue (*arrow*) with enhancement post-contrast (*C*). There is also a macrocystic component in the submandibular region that is bright on fluid-sensitive sequence (*B, arrowheads*), with only peripheral/septal enhancement after contrast (*C*).

arteries and draining veins with the absence of a mass (**Fig. 8**). These can be seen on SE sequences as flow-related signal void or as bright signal on GRE.[8,31] There may be edema and enhancement in the surrounding tissues, although no focal mass is present.[8] Similar to VM, associated soft tissue changes may be present, including fatty infiltration of the adjacent musculature, and prominence of subcutaneous fat compared with the contralateral side.[30] The enlarged feeding arteries, draining veins and nidus with shunt can be confirmed with angiography.[8]

Complications and Treatment

AVM and AVF cause pain and ulceration secondary to ischemia from steal phenomenon. The shunting causes increased cardiac output.[3]

Treatment of AVM is complex. Options include surgery, embolization, or a combination of the two, although complete cure is often not achieved. The treatment is primarily aimed at symptom relief and decreasing deformity. Embolization can be used preoperatively to reduce blood loss, or as primary therapy for lesions not amenable to surgery. Embolization agents include n-butyl cyanoacrylate, Onyx (ev3, Irvine, CA, USA), and ethanol. Surgery offers the best long-term outcome, but recurrence rates are still high, particularly if the AVM is not small and localized. Incomplete excision can lead to worsening of the malformation. The target of treatment should be the nidus of the AVM. It is important that proximal feeding arteries not be ligated with surgery or occluded with embolization because subsequent recanalization and vasculogenesis stimulate enlargement, and access to the nidus would be blocked for future embolization.[46,49]

AVF can be treated by obliterating the anomalous arteriovenous connection, most commonly with coils. As with AVM, occluding the proximal feeding artery leads to poor response.[50]

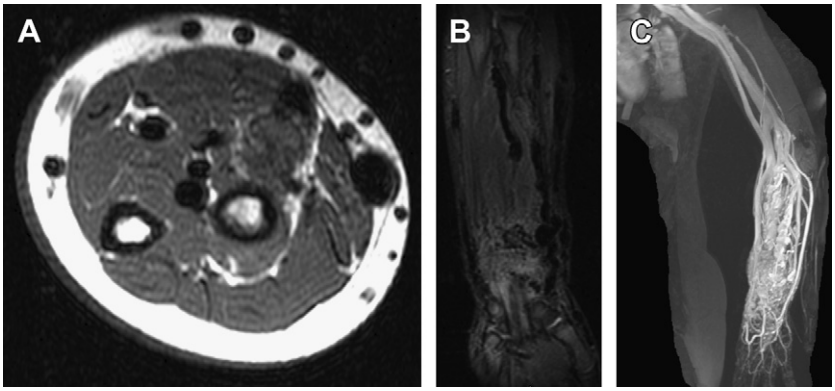

Fig. 8. AVM in left arm of 21-month-old girl. Axial T1 (*A*) and coronal STIR (*B*) images show large flow voids in the subcutaneous tissues and muscles corresponding to dilated arteries and veins. By 8 years of age, the AVM has progressed with markedly dilated, tortuous arteries and veins seen on postcontrast MR angiogram (*C*).

SYNDROMES ASSOCIATED WITH VASCULAR ANOMALIES

Like IH, vascular malformations are also seen in a variety of syndromes, which can be grouped into those containing slow-flow lesions and those with fast-flow lesions. The role of imaging is to delineate the individual fast- or slow-flow components because each entity requires specifically tailored treatment, and to diagnose associated complications.

Slow-Flow Combined Vascular Anomaly Syndromes

Klippel-Trénaunay syndrome

Klippel-Trénaunay syndrome (KTS) affects one lower extremity in 95% of patients and is defined by at least two of the following abnormalities: cutaneous capillary malformations (port-wine stain) of the affected limb; VM or varicose veins; or soft tissue or bony overgrowth of the affected limb.[51,52] The port-wine stain is the most common feature, seen in 98% of patients.[52] KTS is frequently associated with persistent embryologic veins including the lateral vein of the thigh (also known as the marginal vein or the vein of Servelle), and persistent sciatic veins. There may be aplasia or hypoplasia of the lymphatic trunks, with associated lymphedema and cutaneous lymphatic vesicles; anomalies of the deep venous system, including aneurysmal dilatation, duplication, aplasia, and hypoplasia.[51,53–55]

At the orthopedic level, imaging is useful in assessing bony overgrowth, with the affected limb demonstrating increased size longitudinally and circumferentially. The limb overgrowth continues until physeal closure. It is best assessed with radiographs. In the case of lower-extremity involvement, frontal view of the legs from the hips to the ankles can be obtained to assess leg length discrepancy, and aid in possible treatment planning. Soft tissue overgrowth can be assessed by MRI.[56]

The LM and venous anomalies of KTS can be evaluated by the same techniques used for these entities in isolation, namely US, MRI, and venography (**Fig. 9**).

Maffucci syndrome

Maffucci syndrome (MS) is the combination of enchondromas and VM, with bony and vascular lesions usually appearing in childhood. The enchondromas are most common in the hands and feet. There is a significant risk of malignant degeneration to chondrosarcoma with a wide range of reported incidence from 15% to 40%.[56–58] Patient's with MS also have an increased risk of noncartilaginous tumors, which is why the syndrome has been thought of as a generalized mesodermal dysplasia. The overall malignancy risk has been reported from 23% to 100%.[57] Reported neoplastic associations include spindle cell hemangioedotheliomas, ovarian tumors, and fibrosarcoma.[57,59]

In assessing the bony changes of MS, radiographs are particularly helpful to visualize the enchondromas, which appear as lucent expansile bony lesions, demonstrating the ring and arc appearance of cartilaginous matrix (**Fig. 10**A). Rapidly expanding lesions should be followed to assess for evidence of soft tissue mass and cortical destruction, which may indicate malignant degeneration. This can be further assessed by MRI, although biopsy is typically needed for confirmation.

The soft tissue abnormalities of MS are best evaluated by MRI (**Fig. 10**B), although radiographs

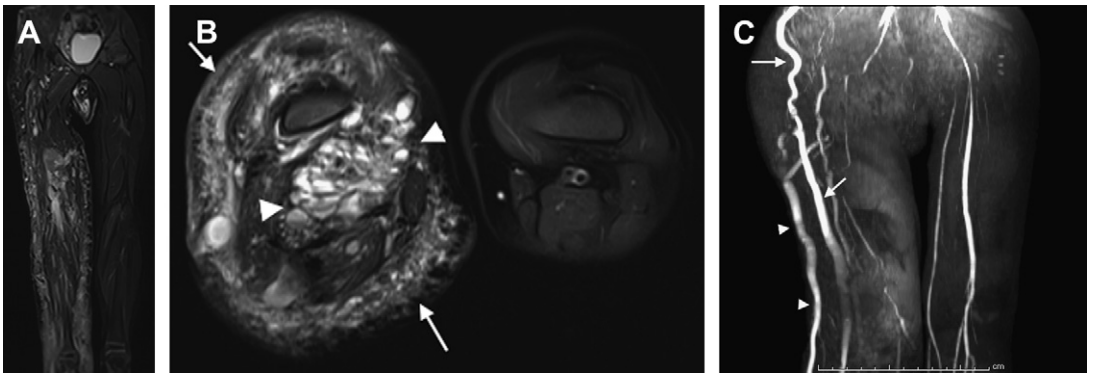

Fig. 9. A 3-year-old boy with KTS who had weeping lymphatic vesicles on the skin. Coronal STIR image of the right lower extremity (*A*) and axial T2 FS image through the distal femur (*B*) demonstrating subcutaneous microcystic LM (*arrows*) and intramuscular VM (*arrowheads*). (*C*) Two-dimensional time-of-flight MR venography shows persistent sciatic vein (*arrows*) and large marginal vein (*arrowheads*).

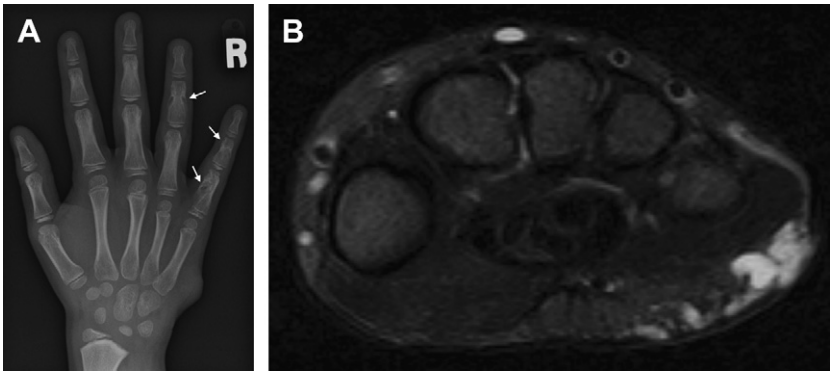

Fig. 10. Maffucci syndrome in a 9-year-old boy. (*A*) Frontal radiograph of the right hand shows lucent bone lesions consistent with enchondromas (*arrows*), and soft tissue mass adjacent to the fifth metacarpal. (*B*) Axial fluid-sensitive sequence demonstrates the mass represents a venous malformation.

may demonstrate phleboliths in the soft tissues related to the VM.

Blue rubber bleb nevus syndrome

This syndrome is characterized by VM that involve the skin and viscera, predominately the gastrointestinal tract.[60] The name comes from the appearance of the skin lesions, which are small (millimeters to 4 cm) bluish protuberances that feel rubbery.[61,62]

The superficial VM can be imaged using US with Doppler, demonstrating the low flow in the lesions; MRI is needed to assess deeper lesions, with potential bone and joint involvement and solid organ involvement (**Fig. 11**).[52] Percutaneous contrast injection of the VM under fluoroscopy is used as a precursor to sclerotherapy in skin lesions.[61] The gastrointestinal tract lesions can be assessed with a variety of modalities, including barium studies, CT, MRI, endoscopy, or video capsule endoscopy. Patients with gastrointestinal VM may have anemia secondary to persistent bleeding and can be treated surgically.[63]

There can be associated skeletal deformity, with pressure effects on the bone from the VM or bony hypertrophy. Joint involvement can cause pain or decreased range of motion.[62]

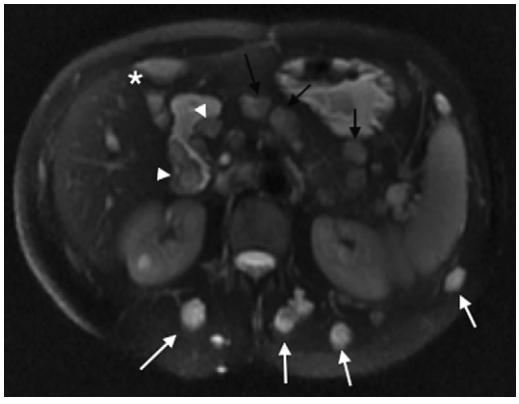

Fig. 11. A 41-year-old woman with blue rubber bleb nevus syndrome. Axial T2 FS image shows lobulated T2 hyperintense lesions in the soft tissues of the back consistent with venous malformations (*white arrows*). There are also gastrointestinal tract VM involving the duodenum (*arrowheads*), visceral malformations of the liver (*asterisk*), and in the peripancreatic region (*black arrows*).

Fast-Flow Combined Vascular Anomaly Syndromes

Parkes Weber syndrome

Parkes Weber syndrome (PWS) must be distinguished from KTS. It is also characterized by cutaneous capillary malformation, with hypertrophy of the affected limb. However, it features AVF, making it a high-flow vascular syndrome lacking the low-flow venous and LM of KTS. The marginal vein of Servelle is not associated with PWS and there tends to be less musculoskeletal involvement.[64]

The AVF of PWS may be imaged using US with Doppler, although it may be challenging to demonstrate the full extent of the lesion. Alternatively, dynamic MRA or digital subtraction angiography can be performed, demonstrating enlarged feeding arteries and early draining veins (**Fig. 12**).[55] Because of the AVF, patients with PWS can have skin ulcerations and high-output cardiac failure, which can be treated with transarterial embolization of the fistula.[55]

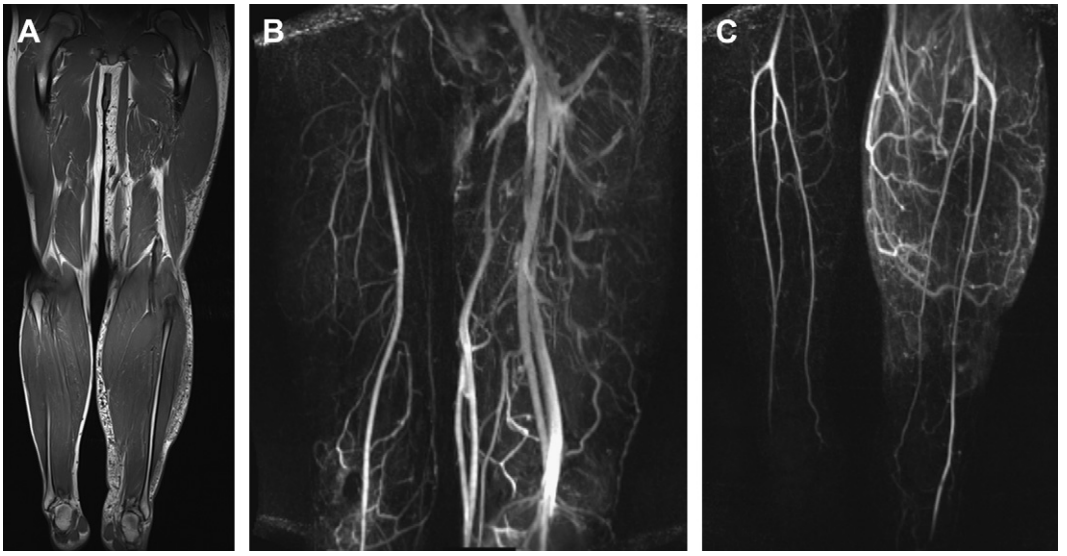

Fig. 12. A 17-year-old boy with Parkes Weber syndrome. (*A*) Coronal T1 image of the legs shows overgrowth of the left leg, affecting soft tissues and bone, with 2 cm measured leg length discrepancy. MR angiogram of the upper (*B*) and lower (*C*) leg show increased size of the arteries of the left thigh compared with the right, and increased size and number of draining veins, which opacify early.

SUMMARY

US and MRI are the most useful imaging modalities in the evaluation of vascular anomalies. The lesions can be accurately characterized by imaging as hemangiomas or malformations, which can be further subdivided into fast flow or slow flow. Key imaging criteria in differentiating the various vascular anomalies include the presence or absence of a soft tissue mass, the flow characteristics of the lesion, and the pattern of enhancement with contrast.

REFERENCES

1. Mulliken JB, Glowacki J. Hemangiomas and vascular malformations in infants and children: a classification based on endothelial characteristics. Plast Reconstr Surg 1982;69:412–22.
2. Dubois J, Alison M. Vascular anomalies: what a radiologist needs to know. Pediatr Radiol 2010;40:895–905.
3. Mulliken JB, Fishman SJ, Burrows PE. Vascular anomalies. Curr Probl Surg 2000;37:517–84.
4. Breugem CC, Maas M, Breugem SJ, et al. Vascular malformations of the lower limb with osseous involvement. J Bone Joint Surg Br 2003;85:399–405.
5. Haggstrom AN, Drolet BA, Baselga E, et al. Prospective study of infantile hemangiomas: demographic, prenatal, and perinatal characteristics. J Pediatr 2007;150:291–4.
6. Dubois J, Patriquin HB, Garel L, et al. Soft-tissue hemangiomas in infants and children: diagnosis using Doppler sonography. AJR Am J Roentgenol 1998;171:247–52.
7. Paltiel HJ, Burrows PE, Kozakewich HP, et al. Soft-tissue vascular anomalies: utility of US for diagnosis. Radiology 2000;214:747–54.
8. Konez O, Burrows PE. Magnetic resonance of vascular anomalies. Magn Reson Imaging Clin N Am 2002;10:363–88, vii.
9. Meyer JS, Hoffer FA, Barnes PD, et al. Biological classification of soft-tissue vascular anomalies: MR correlation. AJR Am J Roentgenol 1991;157:559–64.
10. Burrows PE, Mulliken JB, Fellows KE, et al. Childhood hemangiomas and vascular malformations: angiographic differentiation. AJR Am J Roentgenol 1983;141:483–8.
11. Koplewitz BZ, Springer C, Slasky BS, et al. CT of hemangiomas of the upper airways in children. AJR Am J Roentgenol 2005;184:663–70.
12. Rossler L, Rothoeft T, Teig N, et al. Ultrasound and colour Doppler in infantile subglottic haemangioma. Pediatr Radiol 2011;41:1421–8.
13. Haggstrom AN, Skillman S, Garzon MC, et al. Clinical spectrum and risk of PHACE syndrome in cutaneous and airway hemangiomas. Arch Otolaryngol Head Neck Surg 2011;137:680–7.
14. Frieden IJ, Reese V, Cohen D. PHACE syndrome. The association of posterior fossa brain malformations, hemangiomas, arterial anomalies, coarctation of the aorta and cardiac defects, and eye abnormalities. Arch Dermatol 1996;132:307–11.
15. Iacobas I, Burrows PE, Frieden IJ, et al. LUMBAR: association between cutaneous infantile hemangiomas of

the lower body and regional congenital anomalies. J Pediatr 2010;157:795–801.e1–7.
16. Schumacher WE, Drolet BA, Maheshwari M, et al. Spinal dysraphism associated with the cutaneous lumbosacral infantile hemangioma: a neuroradiological review. Pediatr Radiol 2012;42:315–20.
17. Stockman A, Boralevi F, Taieb A, et al. SACRAL syndrome: spinal dysraphism, anogenital, cutaneous, renal and urologic anomalies, associated with an angioma of lumbosacral localization. Dermatology 2007;214:40–5.
18. Huang SA, Tu HM, Harney JW, et al. Severe hypothyroidism caused by type 3 iodothyronine deiodinase in infantile hemangiomas. N Engl J Med 2000;343:185–9.
19. Mulliken JB, Enjolras O. Congenital hemangiomas and infantile hemangioma: missing links. J Am Acad Dermatol 2004;50:875–82.
20. Enjolras O, Mulliken JB, Boon LM, et al. Noninvoluting congenital hemangioma: a rare cutaneous vascular anomaly. Plast Reconstr Surg 2001;107:1647–54.
21. Gorincour G, Kokta V, Rypens F, et al. Imaging characteristics of two subtypes of congenital hemangiomas: rapidly involuting congenital hemangiomas and non-involuting congenital hemangiomas. Pediatr Radiol 2005;35:1178–85.
22. Krol A, MacArthur CJ. Congenital hemangiomas: rapidly involuting and noninvoluting congenital hemangiomas. Arch Facial Plast Surg 2005;7:307–11.
23. Rogers M, Lam A, Fischer G. Sonographic findings in a series of rapidly involuting congenital hemangiomas (RICH). Pediatr Dermatol 2002;19:5–11.
24. Konez O, Burrows PE, Mulliken JB, et al. Angiographic features of rapidly involuting congenital hemangioma (RICH). Pediatr Radiol 2003;33:15–9.
25. Sarkar M, Mulliken JB, Kozakewich HP, et al. Thrombocytopenic coagulopathy (Kasabach-Merritt phenomenon) is associated with Kaposiform hemangioendothelioma and not with common infantile hemangioma. Plast Reconstr Surg 1997;100:1377–86.
26. Lyons LL, North PE, Mac-Moune Lai F, et al. Kaposiform hemangioendothelioma: a study of 33 cases emphasizing its pathologic, immunophenotypic, and biologic uniqueness from juvenile hemangioma. Am J Surg Pathol 2004;28:559–68.
27. Hermans DJ, van Beynum IM, van der Vijver RJ, et al. Kaposiform hemangioendothelioma with Kasabach-Merritt syndrome: a new indication for propranolol treatment. J Pediatr Hematol Oncol 2011;33:e171–3.
28. Dubois J, Garel L, David M, et al. Vascular soft-tissue tumors in infancy: distinguishing features on Doppler sonography. AJR Am J Roentgenol 2002; 178:1541–5.
29. Chen YJ, Wang CK, Tien YC, et al. MRI of multifocal kaposiform haemangioendothelioma without Kasabach-Merritt phenomenon. Br J Radiol 2009; 82:e51–4.
30. Lopez V, Marti N, Pereda C, et al. Successful management of Kaposiform hemangioendothelioma with Kasabach-Merritt phenomenon using vincristine and ticlopidine. Pediatr Dermatol 2009;26:365–6.
31. Rak KM, Yakes WF, Ray RL, et al. MR imaging of symptomatic peripheral vascular malformations. AJR Am J Roentgenol 1992;159:107–12.
32. Dubois JM, Sebag GH, De Prost Y, et al. Soft-tissue venous malformations in children: percutaneous sclerotherapy with Ethibloc. Radiology 1991;180: 195–8.
33. Trop I, Dubois J, Guibaud L, et al. Soft-tissue venous malformations in pediatric and young adult patients: diagnosis with Doppler US. Radiology 1999;212: 841–5.
34. Dubois J, Soulez G, Oliva VL, et al. Soft-tissue venous malformations in adult patients: imaging and therapeutic issues. Radiographics 2001;21: 1519–31.
35. Laor T, Burrows PE, Hoffer FA. Magnetic resonance venography of congenital vascular malformations of the extremities. Pediatr Radiol 1996;26:371–80.
36. Claudon M, Upton J, Burrows PE. Diffuse venous malformations of the upper limb: morphologic characterization by MRI and venography. Pediatr Radiol 2001;31:507–14.
37. Puig S, Aref H, Chigot V, et al. Classification of venous malformations in children and implications for sclerotherapy. Pediatr Radiol 2003;33:99–103.
38. Cahill AM, Nijs EL. Pediatric vascular malformations: pathophysiology, diagnosis, and the role of interventional radiology. Cardiovasc Intervent Radiol 2011; 34:691–704.
39. Boardman SJ, Cochrane LA, Roebuck D, et al. Multimodality treatment of pediatric lymphatic malformations of the head and neck using surgery and sclerotherapy. Arch Otolaryngol Head Neck Surg 2010;136:270–6.
40. Puig S, Casati B, Staudenherz A, et al. Vascular low-flow malformations in children: current concepts for classification, diagnosis and therapy. Eur J Radiol 2005;53:35–45.
41. Nehra D, Jacobson L, Barnes P, et al. Doxycycline sclerotherapy as primary treatment of head and neck lymphatic malformations in children. J Pediatr Surg 2008;43:451–60.
42. Kern S, Niemeyer C, Darge K, et al. Differentiation of vascular birthmarks by MR imaging. An investigation of hemangiomas, venous and lymphatic malformations. Acta Radiol 2000;41:453–7.
43. Shiels WE II, Kenney BD, Caniano DA, et al. Definitive percutaneous treatment of lymphatic malformations of the trunk and extremities. J Pediatr Surg 2008;43:136–9 [discussion: 40].
44. Yang Y, Sun M, Ma Q, et al. Bleomycin A5 sclerotherapy for cervicofacial lymphatic malformations. J Vasc Surg 2011;53:150–5.

45. Bai Y, Jia J, Huang XX, et al. Sclerotherapy of microcystic lymphatic malformations in oral and facial regions. J Oral Maxillofac Surg 2009;67:251–6.
46. Greene AK, Orbach DB. Management of arteriovenous malformations. Clin Plast Surg 2011;38: 95–106.
47. Kohout MP, Hansen M, Pribaz JJ, et al. Arteriovenous malformations of the head and neck: natural history and management. Plast Reconstr Surg 1998;102:643–54.
48. Lawdahl RB, Routh WD, Vitek JJ, et al. Chronic arteriovenous fistulas masquerading as arteriovenous malformations: diagnostic considerations and therapeutic implications. Radiology 1989;170:1011–5.
49. Do YS, Yakes WF, Shin SW, et al. Ethanol embolization of arteriovenous malformations: interim results. Radiology 2005;235:674–82.
50. Holt PD, Burrows PE. Interventional radiology in the treatment of vascular lesions. Facial Plast Surg Clin North Am 2001;9:585–99.
51. Jacob AG, Driscoll DJ, Shaughnessy WJ, et al. Klippel-Trenaunay syndrome: spectrum and management. Mayo Clin Proc 1998;73:28–36.
52. Elsayes KM, Menias CO, Dillman JR, et al. Vascular malformation and hemangiomatosis syndromes: spectrum of imaging manifestations. AJR Am J Roentgenol 2008;190:1291–9.
53. Bastarrika G, Redondo P, Sierra A, et al. New techniques for the evaluation and therapeutic planning of patients with Klippel-Trenaunay syndrome. J Am Acad Dermatol 2007;56:242–9.
54. Servelle M. Klippel and Trenaunay's syndrome. 768 operated cases. Ann Surg 1985;201:365–73.
55. Ziyeh S, Spreer J, Rossler J, et al. Parkes Weber or Klippel-Trenaunay syndrome? Non-invasive diagnosis with MR projection angiography. Eur Radiol 2004;14:2025–9.
56. Garzon MC, Huang JT, Enjolras O, et al. Vascular malformations. Part II: associated syndromes. J Am Acad Dermatol 2007;56:541–64.
57. Albregts AE, Rapini RP. Malignancy in Maffucci's syndrome. Dermatol Clin 1995;13:73–8.
58. Kessler HB, Recht MP, Dalinka MK. Vascular anomalies in association with osteodystrophies: a spectrum. Skeletal Radiol 1983;10:95–101.
59. Fanburg JC, Meis-Kindblom JM, Rosenberg AE. Multiple enchondromas associated with spindle-cell hemangioendotheliomas. An overlooked variant of Maffucci's syndrome. Am J Surg Pathol 1995;19: 1029–38.
60. Moodley M, Ramdial P. Blue rubber bleb nevus syndrome: case report and review of the literature. Pediatrics 1993;92:160–2.
61. Kassarjian A, Fishman SJ, Fox VL, et al. Imaging characteristics of blue rubber bleb nevus syndrome. AJR Am J Roentgenol 2003;181:1041–8.
62. McCarthy JC, Goldberg MJ, Zimbler S. Orthopaedic dysfunction in the blue rubber-bleb nevus syndrome. J Bone Joint Surg Am 1982;64:280–3.
63. Barlas A, Avsar E, Bozbas A, et al. Role of capsule endoscopy in blue rubber bleb nevus syndrome. Can J Surg 2008;51:E119–20.
64. Redondo P, Aguado L, Martinez-Cuesta A. Diagnosis and management of extensive vascular malformations of the lower limb: part I. Clinical diagnosis. J Am Acad Dermatol 2011;65:893–906 [quiz: 907–8].